«EMR for Inverter-based Resource Power System»

Khanh-Linh Dang
Linh Tran, Thanh Vo-Duy, Minh C.Ta, João Pedro F. Trovão, Bảo-Huy Nguyễn
CTI Lab for Electric Vehicles, Hanoi University of Science and Technology, Vietnam

TRƯỜNG ĐẠI HỌC BÁCH KHOA HÀ NỘI
HANOI UNIVERSITY OF SCIENCE AND TECHNOLOGY

PTN NGHIÊN CỨU XE ĐIỆN
Control Technique and Innovation Laboratory for Electric Vehicles

« PART 1: Introduction»

- IBRs are gaining popularity
- The increasing of IBRs in grid effects the grid's Inertia and Voltage Regulation
- Maintaining the grid stability is crucial

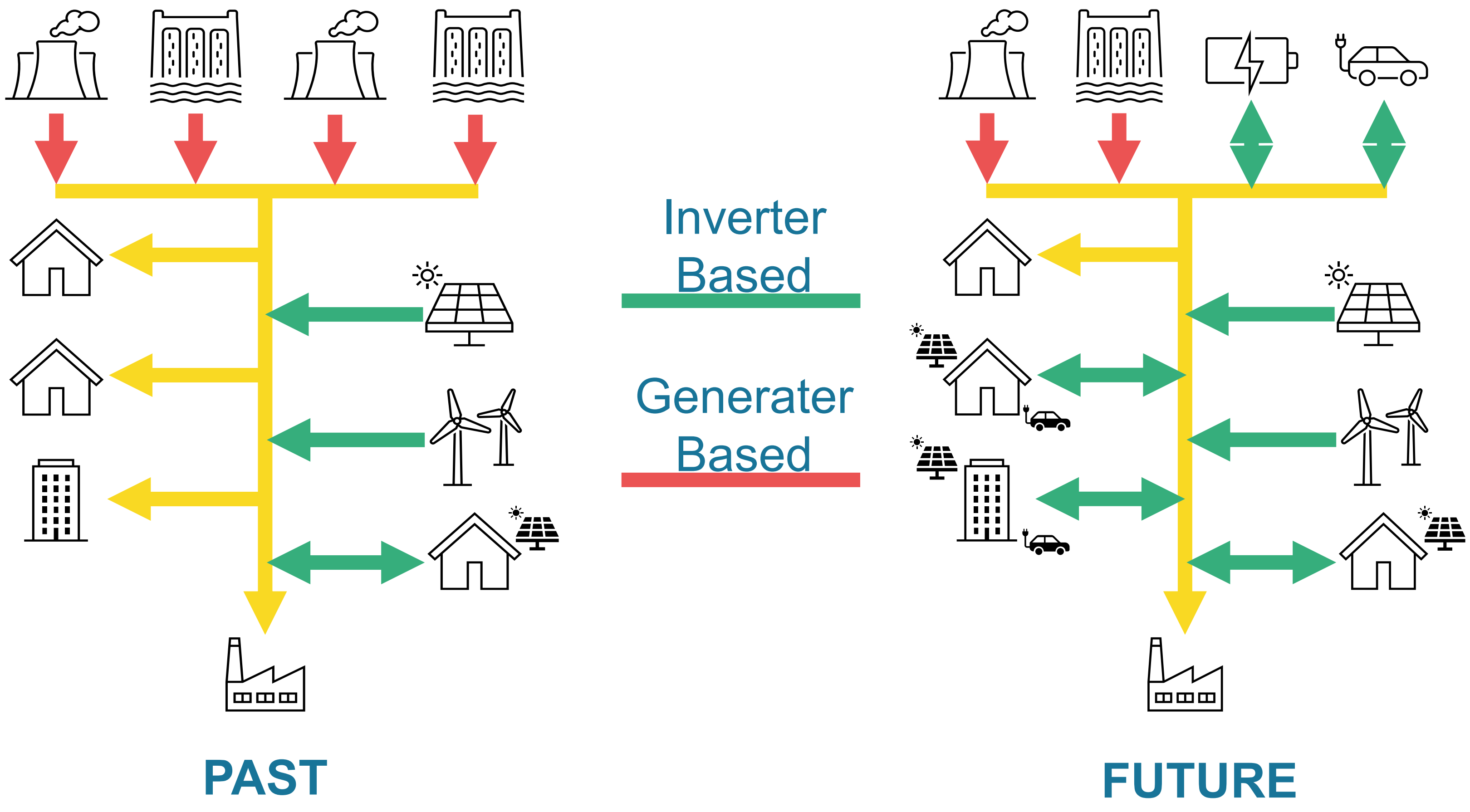

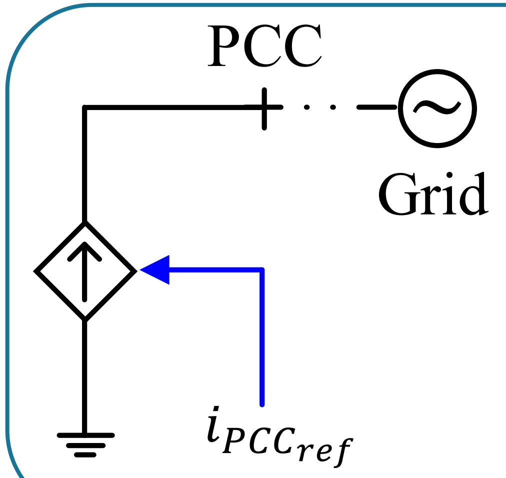

Grid-Following

(Current Source)

Do not directly control voltage-frequency

Cannot work without grid

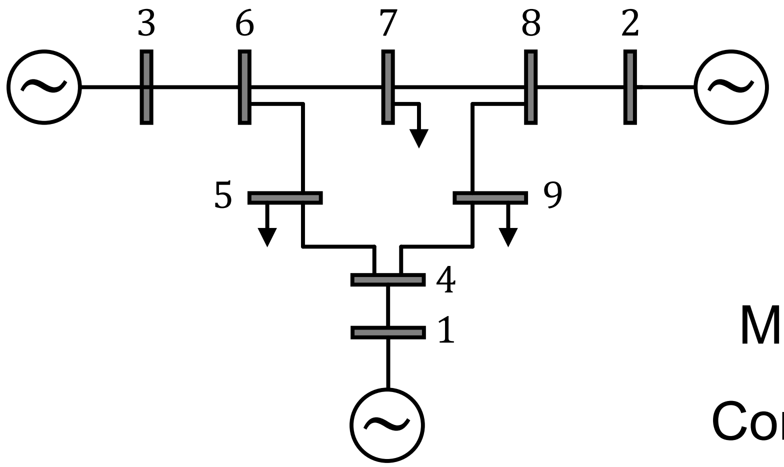

9 BUS

Multi sources

Complex model

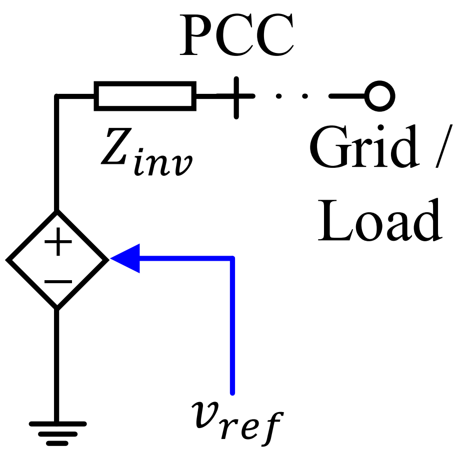

Grid-Forming

(Voltage Source)

Do not directly control of current

Can work in islanded mode

Mathematical Model + Energetic Macroscopic Representation

« PART 2: Single Machine Infinite Bus»

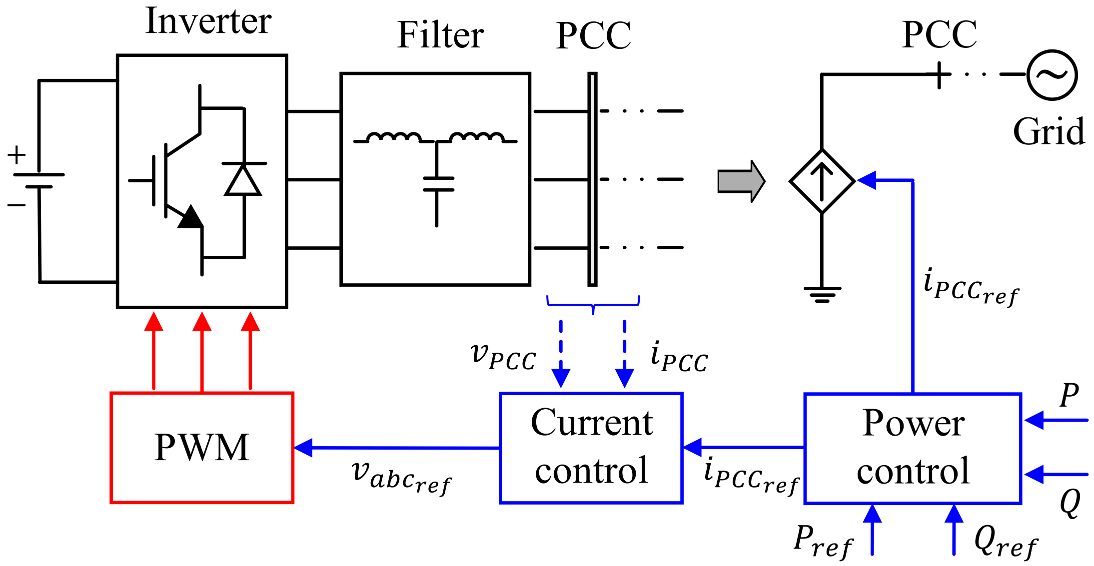

- Cause instability in the grid with high impedance (weak grid)
- Only works in grid connected mode
- Do well with strong grid
- GFLI technique uses Phase-Locked Loop (PLL) for regulation

Table 1. GFLI Fomulas

Phase-Locked Loop (PLL)	$\theta_{PLL} = \frac{1}{s}\left(k_{p_{PLL}} + \frac{k_{i_{PLL}}}{s}\right)(u_{PCC_q} - 0)$	(1)
Active and Reactive power	$P = 1.5\left(u_{PCC_d} i_{PCC_d} + u_{PCq} i_{PCC_q}\right)$ $Q = 1.5\left(-u_{PCC_d} i_{PCC_q} + u_{PCq} i_{PCC_d}\right)$	(2)

With θ_{PLL} is the grid angle, $k_{p_{PLL}}, k_{i_{PLL}}$ are the PLL gains

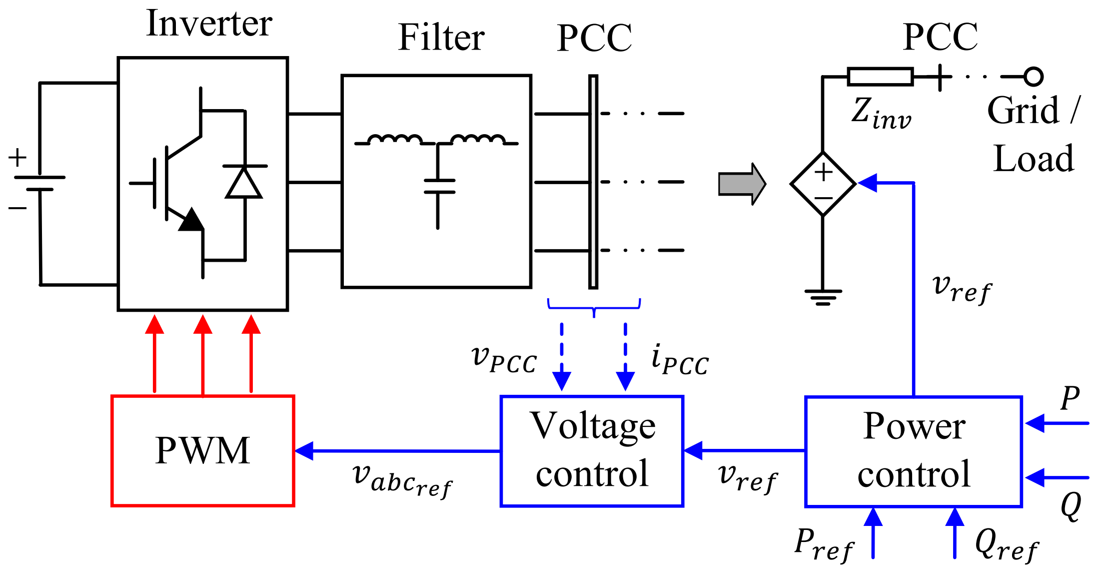

- Sets up the grid voltage magnitude and frequency
- Works in grid connected or islanded mode
- Can work with weak grid
- GFLI technique uses Virtual Synchronous Generator (VSG)

Table 2. GFMI Fomulas

Power synchronization	$J\frac{d\omega_{VSG}}{dt} = \frac{P_{ref} - P}{\omega_{VSG}} - D(\omega_{VSG} - \omega_g)$ $\frac{d\theta_{VSG}}{dt} = \omega_{VSG}$	(3)
Excitation Loop	$E_m = E_0 + k_q \int (k_u(U_N - u_{PCC}) + Q_{ref} - Q)$	(4)

With θ_{VSG} is the grid angle, J, D, E_0, k_q, k_u, U_n are the gains and the coefficient of the algorithm

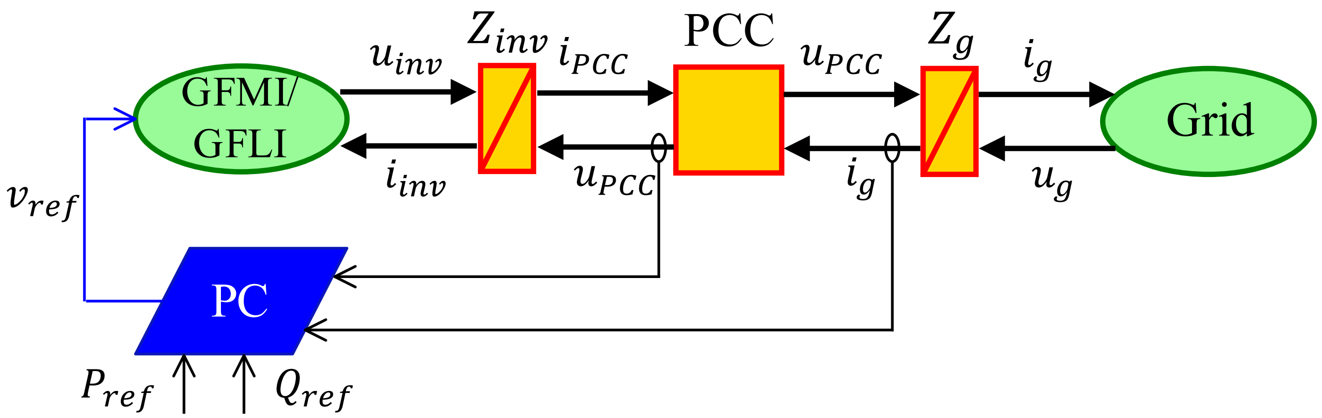

- Each phase of the inverter isconnected with a filter; this filter can be L, LC, or LCL filters
- This model used the controlled voltage source connected to an inductor

Table 3. GFMI Fomulas

Grid impedance	$\frac{u_{PCC} - u_g}{L_g s + R_g} = i_{PCC}$	(5)
PCC Voltage	$u_{PCC}\left(\frac{1}{L_{inv}s + R_{inv}} + \frac{1}{L_g s + R_g}\right) = u_{inv}\frac{1}{L_{inv}s + R_{inv}} + u_g\frac{1}{L_g s + R_g}$	(6)

With $L_g, R_g, L_{inv}, R_{inv}$ is the line and source impedance

« PART 3: Multiple Bus»

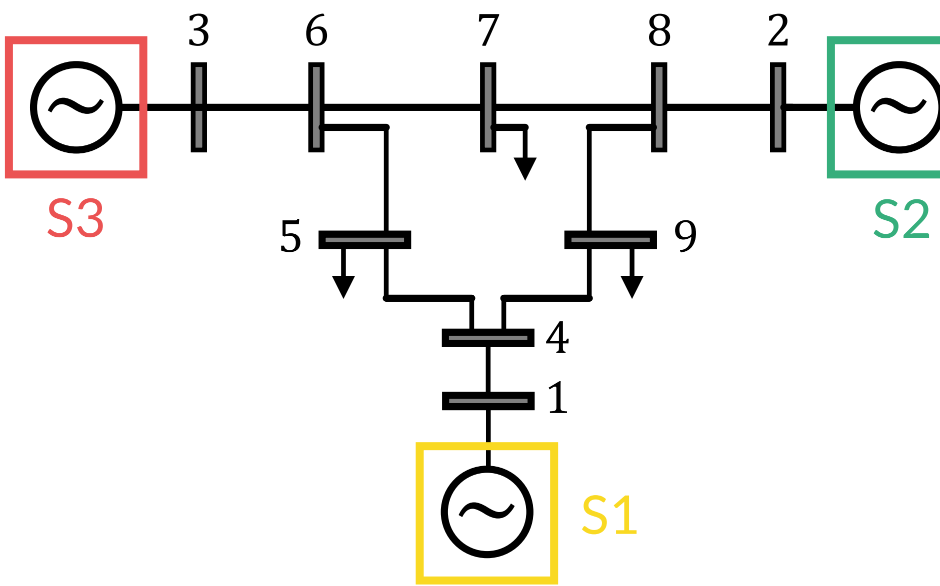

- Source 1: Grid Forming Inverter
- Source 2: Synchronous generator
- Source 3: Grid Following inverter
- BUS 4,5,6,7,8,9
- PCC BUS 1,2,3

Table 4. IEEE 9 Bus Fomulas

PCC Voltage	$u_{PCC}\left(\frac{1}{L_{mn}s+R_{mn}}+\frac{1}{L_ns+R_n}\right) = u_{BUSm}\frac{1}{L_ns+R_n}+u_{gn}\frac{1}{L_ns+R_n}$	(7)
BUS Voltage	$u_{BUS}\left(\frac{1}{L_is+R_i}+\frac{1}{L_js+R_j}+\frac{1}{L_ks+R_k}\right) = u_i\frac{1}{L_is+R_i}+u_j\frac{1}{L_js+R_j}+u_k\frac{1}{L_ks+R_k}$	(8)
Load voltage	$\frac{u_{PCC}}{L_{load}s+R_{load}} = i_{load}$	(9)

With L_x, R_x is the line, load and source impedance

EMR for Inverter-based Resource Power System

Energetic Macroscopic Representation of Multiple Bus

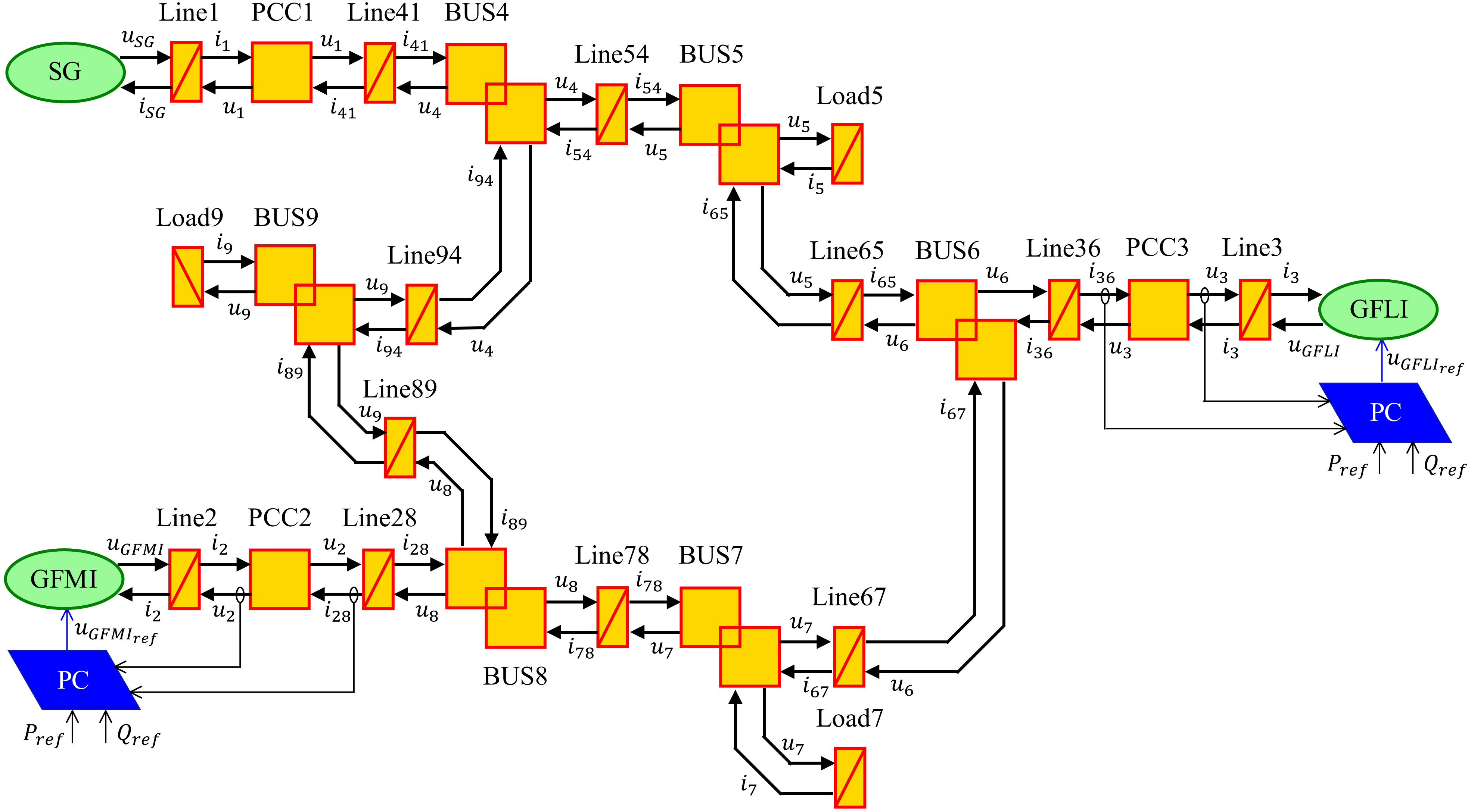

« PART 4: Results and discussions»

Table 5. Simulation parameters

Parameters	**Values**	**Units**
Grid		
Nominal voltage	10	kV
Nominal frequency	50	Hz
Nominal angular speed	314	rad/s
GFLI		
Filter inductance	0.3	mH
Filter resistance	0.115	Ω
GFMI		
Filter inductance	0.3	mH
Filter resistance	0.115	Ω
Line		
Line inductance (Short)	28	mH
Line resistance (Short)	2.3	Ω
Line inductance (Long)	50	mH
Line resistance (Long)	4.0	Ω

- **Simulation parameters:** Table 5
- **Simulation scenarios**: SMIB and Multi Bus
- **SMIB**
  - Scenarios 1: GFLI
  - Scenarios 2: GFMI
  - Initial active power 8MW, then 12MW, 20MW, 24MW after each 10s.
  - Thus the Short Circuit Ratio (SCR) change from 5.48 to 1.83
- IEEE 9BUS: References: 2MW for GFLI and 3MW for GFMI, then change at 10s.

Simulation results

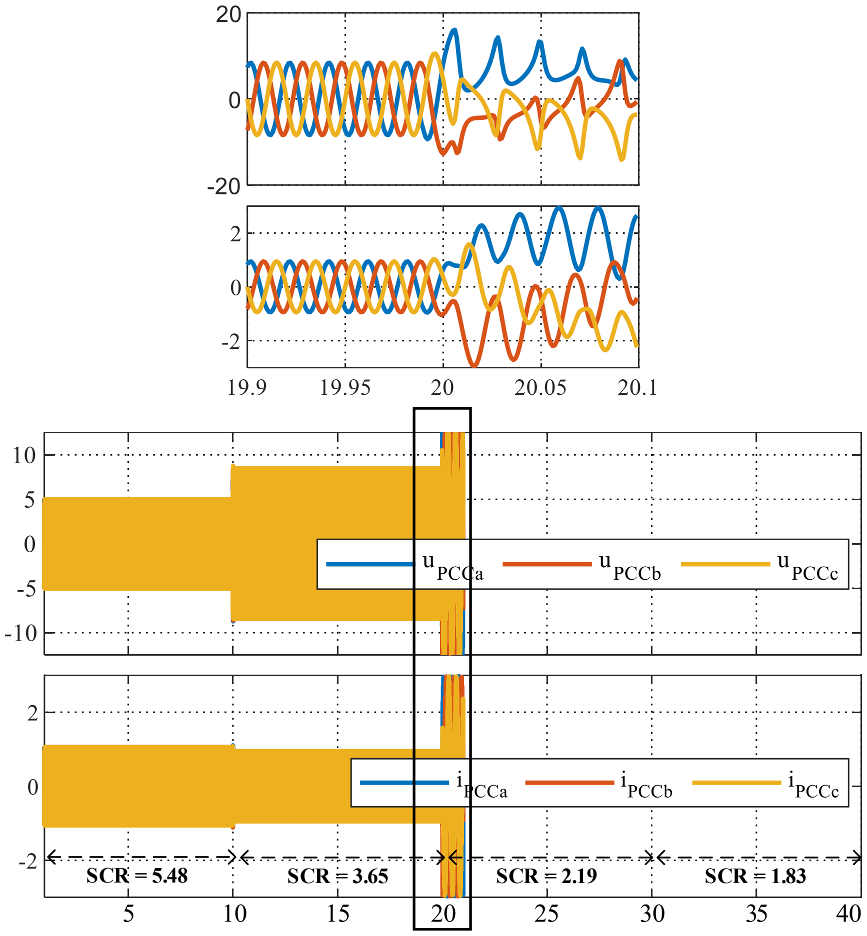

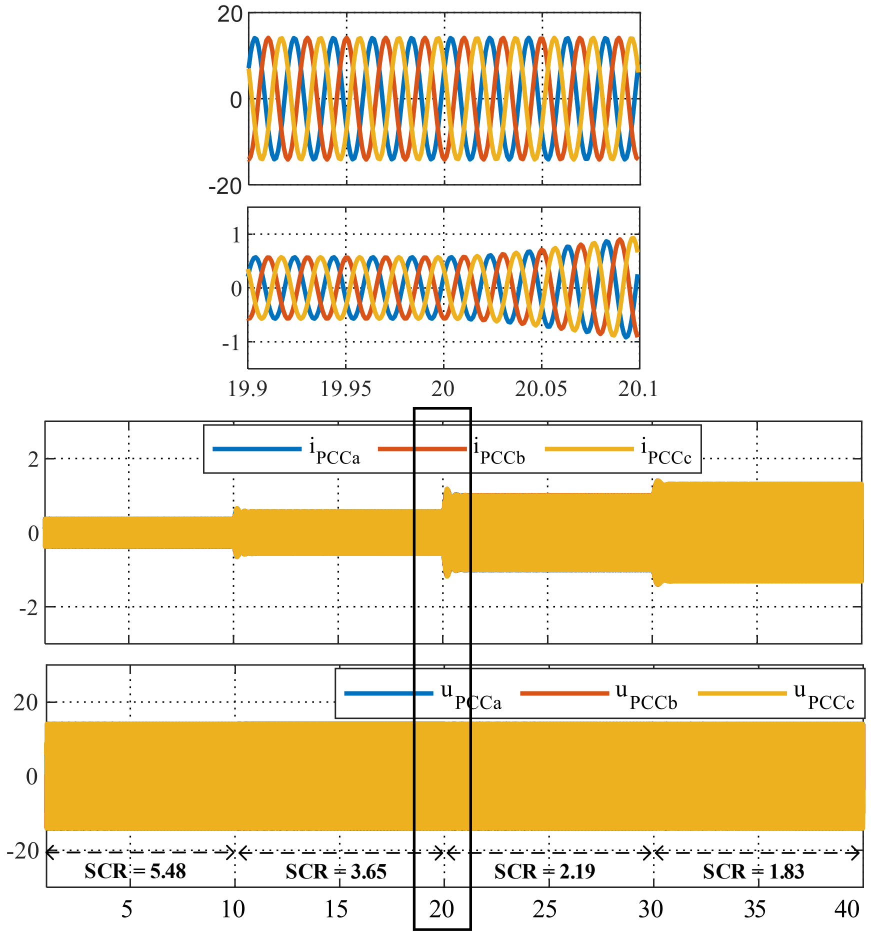

- GFMI performs well at low SCR while the GFLI becomes unstable when the grid is weak

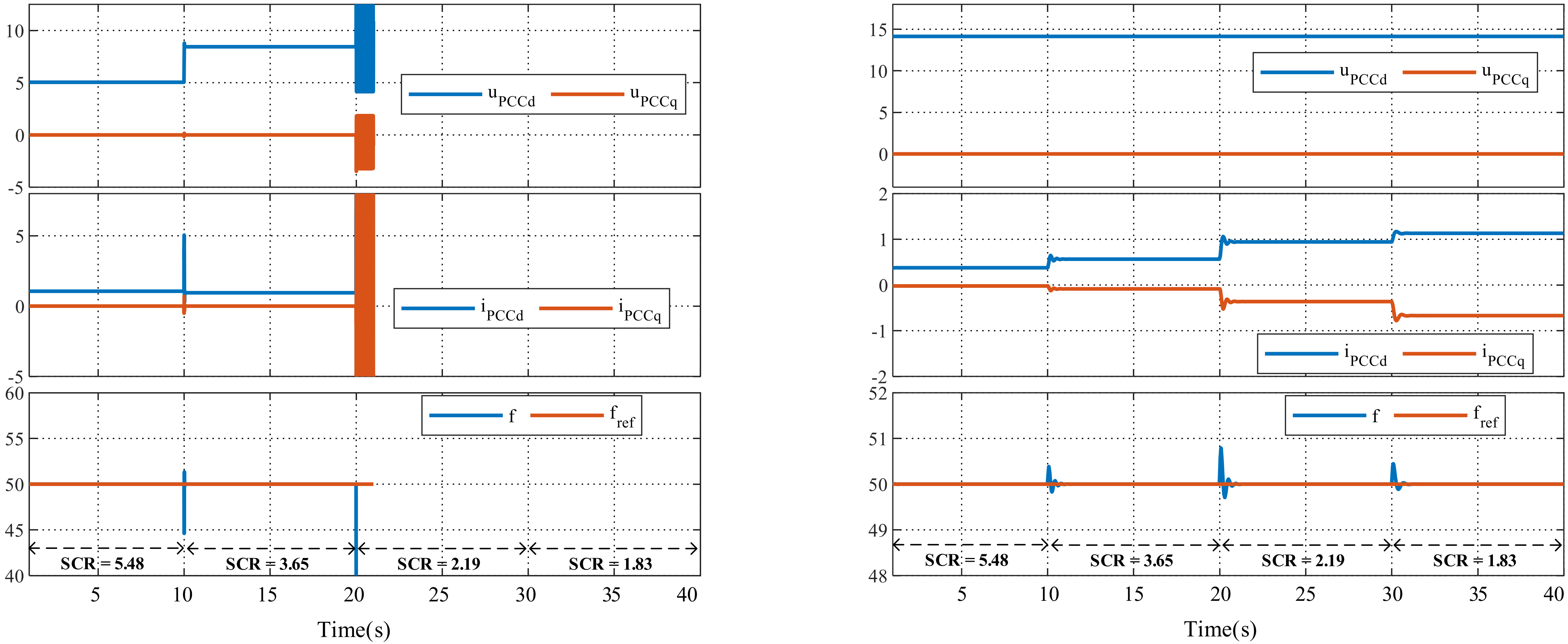

- GFLI voltages and currents vary higher than GFMI

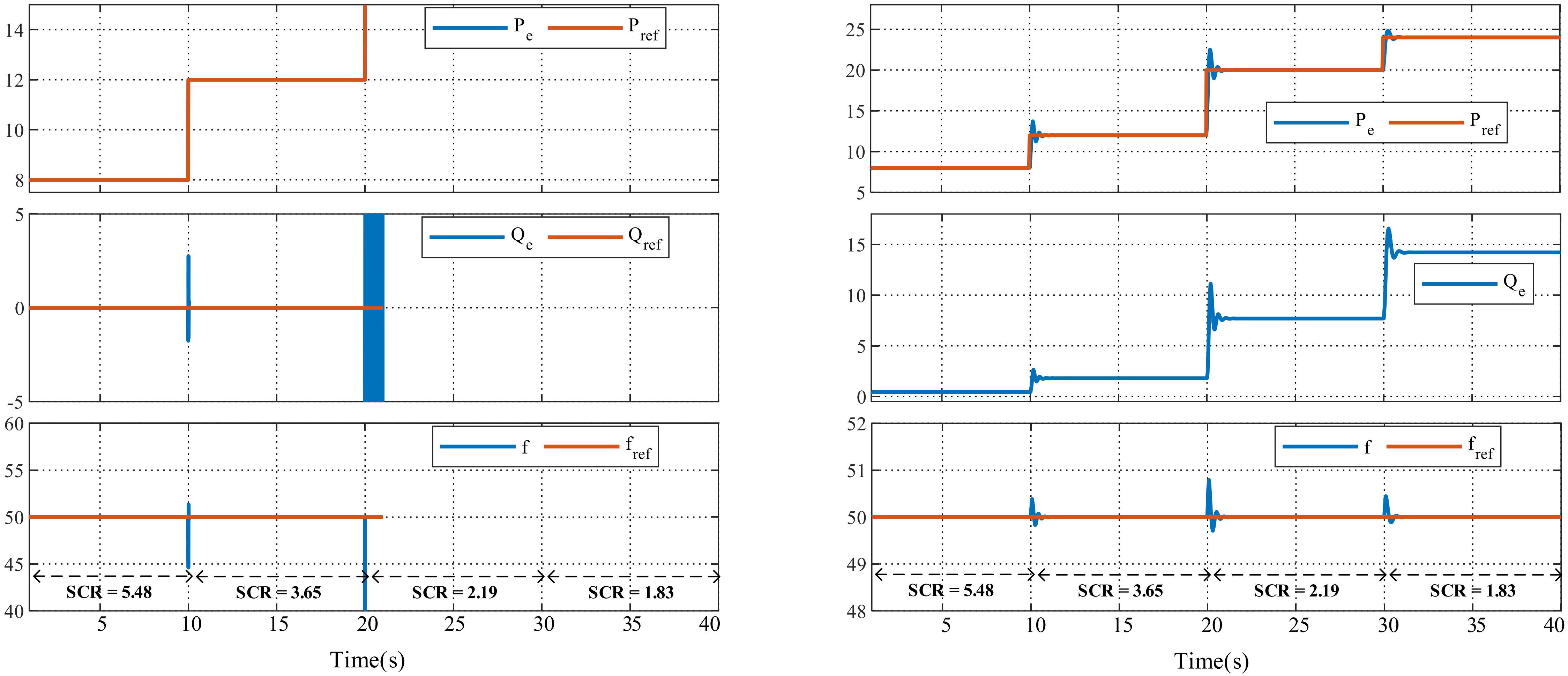

- GFLI frequency varies larger than that of GFMI, which exceeds the range -10% to +10% of 50Hz

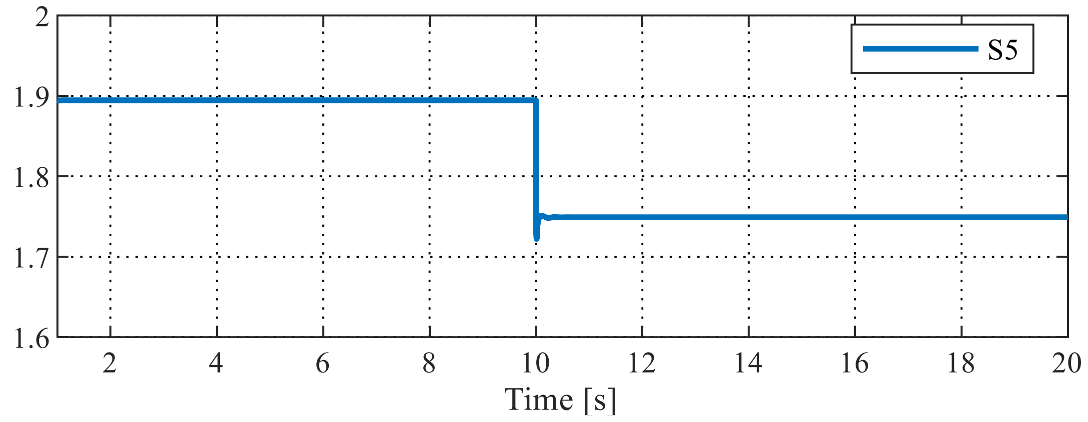

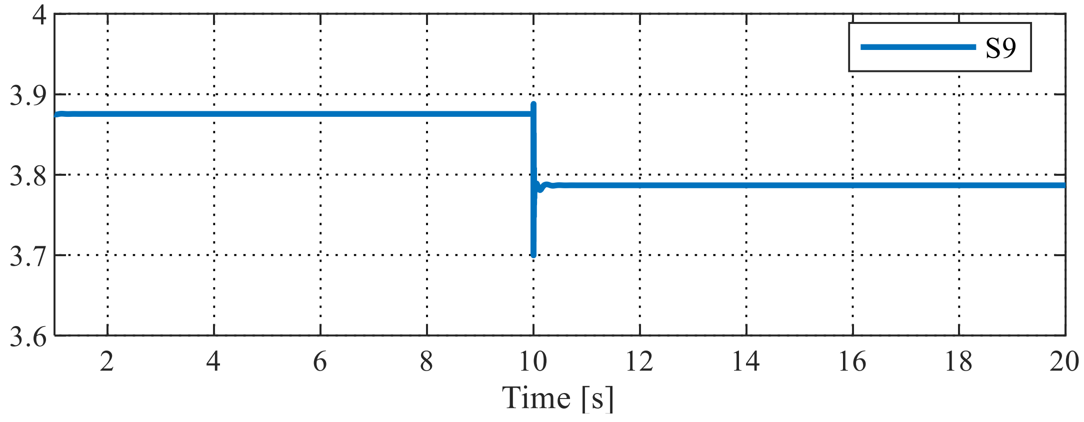

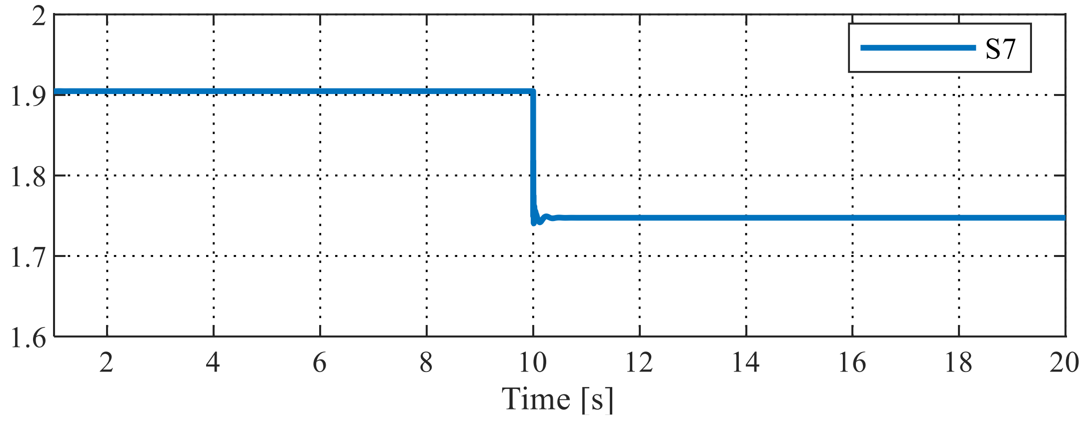

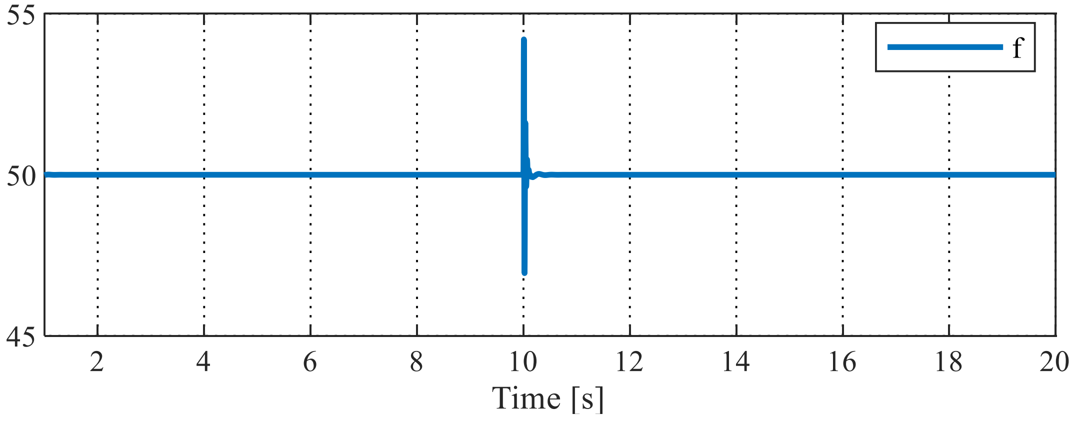

- Frequency response value varies inthe range of 45 to 55 Hz, which is about -10% and +10%.

«CONCLUSIONS»

CONCLUSION

- ❑ Grid forming and following inverter control schemes are investigated
- ❑ Studied with both the SMIB and multi-bus models
- ❑ The simulation shows that the EMR method perfoms well

FUTURE WORK

- ❑ Grid forming and following inverter control schemes in fault scenarios
- ❑ Studied with more bus model
- ❑ Optimal control for fault scenarios

References

[1] Lin, Yashen, Ho, Joseph H., Johnson, Brian B., Flicker, Jack D., Lasseter, Robert H., Villegas Pico, Hugo N., Sen, Gabi-Sa., Pierre, Brian J., and Ellis, Abraham. *Research Roadmap on Grid-Forming Inverters*. United States: N. p., 2020. Web. doi:10.2172/1727177.

[2] K. S. Sajadi, P. H. Flisel, M. C. Raza, and J. Uemura, "Energetic macroscopic representation (EMR): New approach for multiphysics mechatronic driving forces," *IFAC Proc. Vol.*, vol. 8, no. PART 1, pp. 773-778, 2012. doi:10.3182/20120912-4-FR-2041.00216.

[3] N. Al Ghamdi, S. B. Wang, E. Lorenz, and M. Schuerlein, "Energetic macroscopic representation and inversion-based control of DC microgrid," 2013 *15th Eur. Conf. Power Electron. Appl. EPE*, 2013, no. September, 2013, doi: 10.1109/EPE.2013.6634368.

[4] A. Koita, A. Payman, B. Dakyo, and D. Hissel, "Control of a Wind Energy Conversion System using the Energetic Macroscopic Representation," *7th Int. IEEE Conf. Renew. Energy Res. Appl. ICRERA*, 2018, pp. 1460-1465, 2018. doi: 10.1109/ICRERA.2018.8566874.

[5] D. Prabhakaran, M. H. Lasseter, and T. M. Jahns, "Comparison of Grid Following and Grid Forming Control for a High Inverter Penetration Power System," *2018 IEEE Power and Energy Society General Meeting (PESGM)*, Portland, OR, USA, 2018, pp. 1-5. doi: 10.1109/PESGM.2018.8586162.

[6] U. T. Yaqoob and M. D. Solanki, "Comparison of LCL and LTI filters for inverter interfacing applications," *2017 International Conference on Trends in Electronics and Informatics (ICEI)*, Tirunelveli, India, 2017, pp. 455-458. doi: 10.1109/ICOEI.2017.8300844.

[7] D. Prabhakaran, M. H. Lasseter, and T. M. Jahns, "Comparison of Grid Following and Grid Forming Control for a High Inverter Penetration Power System," *2018 IEEE Power and Energy Society General Meeting (PESGM)*, Portland, OR, USA, 2018, pp. 1-5. doi: 10.1109/PESGM.2018.8586162.

[8] Salem O. Alqarni, H. Karimifard, M. A. A. GFM-based Inverter Control for Power Sharing in Microgrids Based on PM and OV Droop Characteristics. *Sustainability*, 2023; 15(5):11774.

[9] Moattamed, Nabil, Adil A. Muhammad and Chobokar, Mahdi and Fleischer, John. (2023). Accurate circuit of virtual oscillator controlled islanded AC microgrids. *Electric Power Systems Research*. 214. 107987. 10.1016/j.epsr.2022.107987.

[10] Sorawit Hem, Carla Rechan, M. Hossny. *GFM control for a grid-forming converter operating as virtual synchronous generator with enhanced dynamic response capability*. International Journal of Electrical Power and Energy Systems, vol. 149, 10-SsN-11022-0151-6. doi:10.1016/j.ijepes.2023.110779.

[11] U. T. Yaqoob and M. D. Solanki, "Comparison of LCL and LTI filters for inverter interfacing applications," *2017 International Conference on Trends in Electronics and Informatics (ICEI)*, Tirunelveli, India, 2017, pp. 455-458. doi: 10.1109/ICOEI.2017.8300844.

[12] X. Gao, X. Duan, A. Al-Mohtaseb, and F. Blaabjerg, "A Comparative Stability Study of Grid-Following and Grid-Forming Control Schemes in Power Electronic-Based Power Systems," *Power Electron. Drives*, vol. 8, no. 1, pp. 1-20, 2023. doi: 10.2478/pead-2023-0001.

Thanks for your attention !